applied sciences

MDPI

Article

Numerical Simulation and Experimental Verification of Quality Detection of Grouting in Pre-Stressed Pipelines Based on Transmission Wave Method

Qingshan Wang [1], Yun Luo [2], Yang Liu [1,3], Minghao Song [4], Heng Liu [4,*] and Xiaoge Liu [4]

1 China Construction Seventh Engineering Division Co., Ltd., Zhengzhou 450000, China; wangqingshan87@163.com (Q.W.); slyujt@163.com (Y.L.)
2 Yunnan Jiaohang Engineering Technology Co., Ltd., Anning 650300, China; jiaoto2024@163.com
3 China Construction Seventh Engineering Division (Shanghai) Co., Ltd., Shanghai 200001, China
4 School of Water Conservancy and Transportation, Zhengzhou University, 100 Kexue Avenue, Zhengzhou 450001, China; slxy2024a@163.com (M.S.); liuxiaoge2022@163.com (X.L.)
* Correspondence: liuheng88@zzu.edu.cn

Abstract: The quality of grouting in pre-stressed pipelines plays a critical role in ensuring the safety and durability of pre-stressed concrete bridges. In this study, the transmission wave method was proposed as a means to assess the quality of grouting in pre-stressed pipelines. The ABAQUS finite element simulation (FE simulation) method was used to study the propagation of hammer stress waves in pre-stressed pipes. A full-scale test was conducted to verify the numerical simulation using the AGI-BWG instrument system developed to detect the quality of grouting. The results show that the propagation speed of transmitted waves increases and the frequency shifts towards higher frequencies with an increase in void length within pre-stressed pipelines. This research suggests that the propagation velocity of elastic waves in pre-stressed pipelines serves as a key indicator of grouting quality. The transmission wave method, based on hammer signals, proves to be an effective tool for detecting the quality of grouting in pre-stressed pipelines.

Keywords: pre-stressed pipes; transmission wave method; grouting quality; finite element simulation; full-scale test

Citation: Wang, Q.; Luo, Y.; Liu, Y.; Song, M.; Liu, H.; Liu, X. Numerical Simulation and Experimental Verification of Quality Detection of Grouting in Pre-Stressed Pipelines Based on Transmission Wave Method. *Appl. Sci.* **2024**, *14*, 3773. https://doi.org/10.3390/app14093773

Academic Editor: Norhisham H. Bakhary

Received: 12 March 2024
Revised: 24 April 2024
Accepted: 26 April 2024
Published: 28 April 2024

1. Introduction

In recent years, pre-stressed concrete structures have been widely used in large bridge structures due to their significant technical and economic advantages. They are particularly favored by the engineering community for post-tensioned, pre-stressed concrete bridges due to their high strength, large span, lightweight structure, and strong crack resistance. During the production process of pre-stressed beams, pipeline grouting can not only isolate the pre-stressed steel bars from the air, making them less prone to rusting, but it can also generate a good bonding force with the pre-stressed steel bars. By transmitting the load force of the structure through the slurry, the overall integrity of the structure improves, thereby improving the crack resistance and bearing capacity of the components. Poor-quality grouting in pre-stressed pipelines can lead to the corrosion of steel strands, which has a significant impact on the safe bearing capacity and service life of pre-stressed structures and, subsequently, leads to safety accidents, such as bridge collapse. Therefore, conducting research on the detection and evaluation of grouting quality in pre-stressed pipelines has great engineering application value. Damage detection, such as through drilling and slicing, not only causes damage to the pre-stressed steel bars inside the pipelines but also has high costs and low efficiency. Non-destructive testing technology has become a key research direction for pipeline grouting quality inspection due to its advantages, such as its non-destructive nature, compatibility, and dynamism [1].

In terms of non-destructive testing technology research, Martin et al. [2] used the travel time information of ultrasound to invert the internal velocity of concrete specimens and detect voids in pre-stressed pipes. Conner et al. [3] used ground-penetrating radar to detect a reinforced concrete slab containing plastic corrugated pipes, and the results showed that the ground-penetrating radar method could successfully detect defects. Tinkey and Olson [4] conducted testing and research on a full-scale prefabricated U-shaped beam, a solid bridge, large-sized concrete slabs, and five concrete slabs. The results showed that the impact-echo scanning results were consistent with the actual defects, and they further showed that the most significant indication of the existence of voids was a decrease in thickness frequency or an increase in back-calculated thickness values. Brachelet et al. [5] used the magnetic induction heating method to heat concrete specimens and identify areas without grouting. H. K. Chai [6] pointed out that X-ray imaging is effective for detecting the degree of grouting voids and anchor cable corrosion in pre-stressed beams. Ohtsu et al. [7] used the SIBIE (stack imaging of spectral amplitude based on impact-echo) method to detect the grouting status of pipelines in a pre-stressed concrete slab and surface cracks in the peeling area of the concrete pier surface, and the results verified the applicability of the SIBIE method. OSAWA et al. [8] conducted experimental studies on two types of pipeline specimens, metal and plastic, using ultrasonic velocity tomography. The results showed that ultrasonic velocity tomography can identify different degrees of grouting defects in pre-stressed pipelines. Jiangbo Lu [9] established a three-dimensional finite element model using ANSYS/LS-DYNA and analyzed the influence of various parameters, such as the bellows type, hole thickness ratio, and wall thickness ratio, on the thickness frequency at the fully empty channel. Zhiqian Guo [10] used ABAQUS 2020 version software to conduct numerical simulation research on the propagation of chirp signals in pre-stressed pipelines with different grouting degrees. Hani Freij et al. [11] used Gamma Ray Tomography (GRT) to validate experimental pipelines with steel strands and grouting voids, unhydrated grouting, and excess water. The results indicated that GRT can detect complete voids, external voids, and unhydrated grouting, but it has difficulty in detecting smaller internal voids. Shaoqiang Wang [12] established pre-stressed duct models under different working conditions based on ABAQUS software and combined them with the relevant theory of the impact-echo method to study the impact of different pipeline materials, diameters, knocking forces, numbers of steel strands, signal excitations and reception positions, and defect positions on qualitative detection. Water defects, void defects, and slurry water mixing defects were also analyzed, as well as the influence of the number of steel strands and the position of steel bars on positioning detection. The feasibility of utilizing the acoustic emission (AE) technique for mechanical diagnosis and the delamination characterization of fiber-reinforced polymer (FRP)-reinforced concrete structures has been extensively studied. Li, WJ et al. [13] conducted experimental research on this topic, investigating the application of the AE technique in assessing debonding in FRP-reinforced concrete.

In the study of the grouting quality of pre-stressed pipelines, scholars at home and abroad have achieved certain application results by using the core drilling method, X-ray imaging method, impact-echo method, ground-penetrating radar method, ultrasonic waves, and other detection methods. However, there are still some problems in detection accuracy and detection efficiency, i.e., the original structure is damaged, the economic cost is expensive, it is unsafe, the test takes a long time, the metal bellows cannot be detected, and the plastic bellows cannot be detected.

Zhu Ziqiang et al. [14] demonstrated the potential application of the multi-channel ultrasonic transmission method in the quality detection of grouting in pre-stressed metal pipelines through a theoretical analysis and a numerical simulation. In this paper, a method for quickly characterizing the degree of defects using the longitudinal transmission wave method is proposed, and a finite element simulation and full-scale verification tests are carried out. The proposed method combines the advantages of low economic cost, high detection efficiency, simple operation, small impact of the monitored environment, and non-destructive testing, and it is of great scientific significance in the grouting quality testing of pre-stressed pipelines. In Section 1, the preparations of the test samples and transmission wave methods are described. In Section 2, the ABAQUS finite element simulation method is described. In Section 3, an analysis and a comparison of the experimental results are presented.

2. Test Samples and Methods

2.1. Preparations of Experimental Samples

In this study, the process of producing a pre-stressed beam model includes the following steps. Firstly, a steel reinforcement framework is constructed, then a pre-stressed duct is embedded (corrugated pipe), and grouting defect channels and internal defects are set up in the beam. Subsequently, the concrete is pre-molded before pouring, and after it is poured, it is allowed to solidify; then, the beam formwork is removed. Next, the grouting defect pipes are cut off, steel strands and anchorages are installed, pre-stress is applied, the pre-stressed ducts are grouted, and, finally, the cement slurry is cleaned at the grouting defect locations. Upon completion of the entire process, the production of the pre-stressed bridge beam model is successfully achieved. An overall diagram of the pre-stressed bridge beam model is shown in Figure 1.

Figure 1. Overall view of pre-stressed bridge beam model.

Shakor et al. [15]. utilized inkjet 3D printing technology for the fabrication of cement mortar specimens. The performance, structure, and properties of the inkjet 3D-printed cement mortar specimens were investigated through the combination of an experimental analysis and a numerical simulation. These properties were subsequently employed for finite element analysis (FEA) modeling. In this paper, the material properties of the experimental samples are defined as shown in Table 1.

Table 1. Material properties of experimental samples.

Material	Density ρ kg/m^3	Elastic Modulus E Pa	Poisson's Ratio μ
C30 concrete	2360	3×10^{10}	0.2
Mortar	2360	3×10^{10}	0.2
Metal corrugated pipe	7800	21×10^{10}	0.3
Steel strand	7800	21×10^{10}	0.3

The pre-stressed bridge beam slab model was pre-set with four pre-stressed pipes numbered N1, N2, N3, and N4 from top to bottom. There were three defects with a length of 0.5 m in the four pipes. Two of these were located at a distance of 4.25 m to 4.75 m and 6.25 m to 6.75 m in the N1 pipe from the A end. Another was located at a distance of 3.25 m to 3.75 m in the N2 pipe from the A end. Except for the pre-set grouting defects, the N1 and N2 pipelines were densely grouted at other positions. The N3 pipeline was fully grouted, while the N4 pipeline was completely empty and not grouted. A model is shown in Figures 2 and 3.

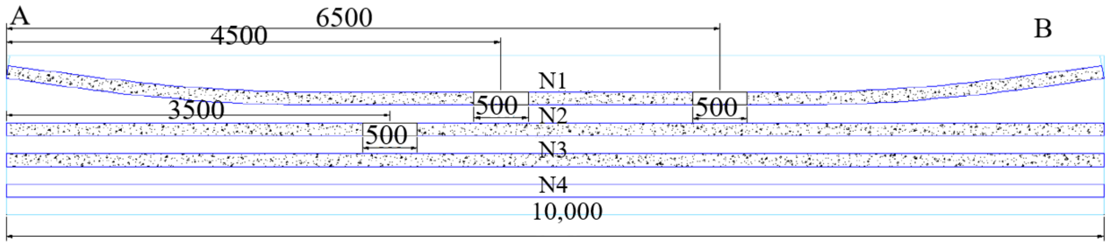

Figure 2. Model design drawing of pre-stressed beam (unit: mm).

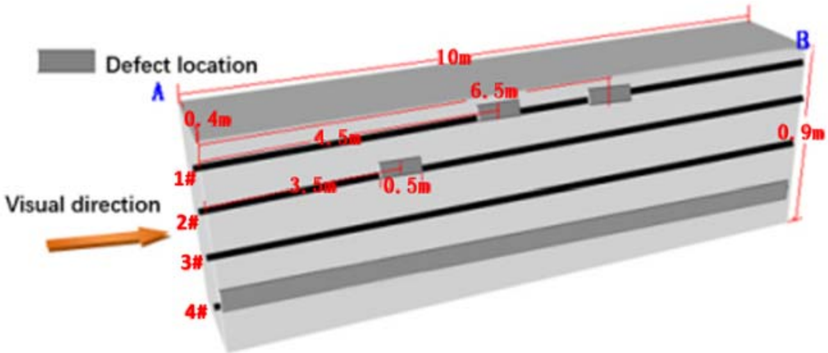

Figure 3. Model diagram of pre-stressed beam (unit: m).

2.2. Transmission Wave Method

In this study, the transmission wave method was used. The transmission wave method is a rapid qualitative inspection method in the longitudinal direction, and it allows for a quick evaluation of the grouting quality of pre-stressed pipelines in a short period of time. For engineering structures, such as box girders, T-beams, and beam slabs, if the two anchoring ends of the pre-stressed pipelines in the beam body are not sealed, the reflection method can be used to detect the grouting quality of the pre-stressed pipelines, thus determining the quality of the grouting.

The principle of transmission method detection is shown in Figure 4. One detector is fixed to each anchor exposed at both ends of the corrugated pipe. At one end (the transmitting end) of the beam plate, a known source signal (hammering signal) is excited and triggered by a detector at that end for timing. When the signal propagates to the other end (the receiving end), it is received by another detector. A signal analysis of the receiving end signal can be carried out separately, and the characteristic values of the hammering signal, such as the wave velocity, energy attenuation, and frequency change, can be obtained [16]. The relationship between the wave velocity, energy attenuation, and frequency change and the grouting compactness can be established to evaluate the grouting compactness.

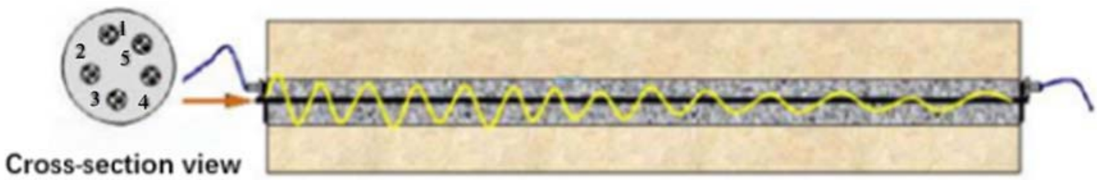

Figure 4. Schematic diagram of transmission wave method.

In this study, the AGI-BWG tester was employed. The AGI-BWG pre-stressed pipeline grouting quality detector [17] is a sophisticated system designed for monitoring and assessing the quality of grouting in pre-stressed pipelines. This detector comprises several essential components that work together seamlessly to ensure accurate data collection and analysis, as shown in Figure 5. The key components of the detector system are as follows:

(1) Computer Processing Terminal: The computer processing terminal serves as the central hub for data processing and analysis. It receives raw data from the wireless data acquisition device, processes and interprets the data, and generates meaningful insights for further action.
(2) Wireless Data Acquisition Device: The wireless data acquisition device is responsible for wirelessly capturing data from the acceleration sensor and transmitting them to the computer processing terminal. This device enables the real-time monitoring of grouting quality parameters, facilitating prompt decision making based on the collected data.
(3) Coding Signal Transmitter: The coding signal transmitter plays a crucial role in transmitting coded signals from the acceleration sensor to the wireless data acquisition device. This component ensures seamless communication between the sensor and the data acquisition unit, enabling accurate data transmission.

Figure 5. AGI-BWG pre-stressed pipeline grouting quality inspection instrument: 1—wireless data acquisition instrument; 2—iPad; 3—signal transmitter; 4—acceleration transducer; 5—wireless router.

Acceleration Sensor (JM Series IEPE-Type Sensor): The acceleration sensor used in the detector is from the JM series IEPE-type sensor family, known for its high sensitivity of 1200 mv/g. This sensor is instrumental in detecting and measuring the acceleration levels experienced by the pipeline, providing valuable data for assessing the structural integrity and grouting quality.

Wireless Router (TP-LINK 150M Wireless Portable Router): The wireless router employed in the system is a TP-LINK 150M wireless portable router. It establishes wireless communication links between the components of the detector system. The effective communication distance between the router and the computer is 70 m, while the limited communication distance between the router and the wireless acquisition device is 30 m.

By leveraging the wireless communication capabilities of the components, the AGI-BWG pre-stressed pipeline grouting quality detector can effectively operate within a detection site with a wireless communication range of up to 100 m. This setup ensures the reliable and efficient monitoring of grouting quality parameters in pre-stressed pipelines, enabling proactive maintenance and quality control measures based on a real-time data analysis.

3. FE Simulation

This study selected the ABAQUS/Explicit module to simulate the hammer impact on the model beam and analyze the propagation characteristics of the hammer wave in the model beam.

3.1. ABAQUS Assumption Model

In the ABAQUS modeling analysis, in order to save computational time and simplify the analysis process, the following assumptions were introduced:

(1) The materials, such as concrete and steel bars, are isotropic and homogeneous linear elastic materials, and they maintain linear elasticity throughout the loading process;
(2) The boundary between elements is continuous;
(3) The calculation of dynamic equations does not consider the influence of gravity;
(4) The model is not subject to any external constraints;
(5) The hammering load is approximately a half-cycle sine load.

To simulate an actual pre-stressed beam, a model beam with a length of 10 m, a height of 0.9 m, and a width of 0.4 m was constructed, with four built-in pre-stressed tendons. For the convenience of calculating and simplifying the model, five steel strands were combined into a bundle with a radius of 17 mm and a length of 10.02 m. At the same time, a mortar with a length of 10 m and a radius of 55 mm was injected around the steel strands, with 0.01 m of the steel strands exposed at both ends of the mortar. All pipes were made of a metal corrugated tube material with a thickness of 1 mm. For the internal model of the 10.02 m steel strand pipeline, ① mortar with a length of 10 m and a radius of 55 mm was injected into pipeline 1 and the void of 0.5 m at 4.25 m~4.75 m and 6.25 m~6.75 m, respectively. ② Mortar with a length of 10 m and a radius of 55 mm was injected into pipeline 2 and the void of 0.5 m at a distance of 3.25 m to 3.75 m. ③ Mortar with a length of 10 m and a radius of 55 mm was injected into pipeline 3. ④ Pipeline 4 was not filled with mortar. The grid size was set to 5 mm, the grid unit type was C3D8R, and the unit type was hexahedron. The material properties are in Section 2.1. A model diagram of the modeled rear beam is shown in Figures 6 and 7.

Using a half-sine periodic load, as shown in Figure 8, the maximum concentrated force was 100 N, and the duration of the impact action was 30 μs.

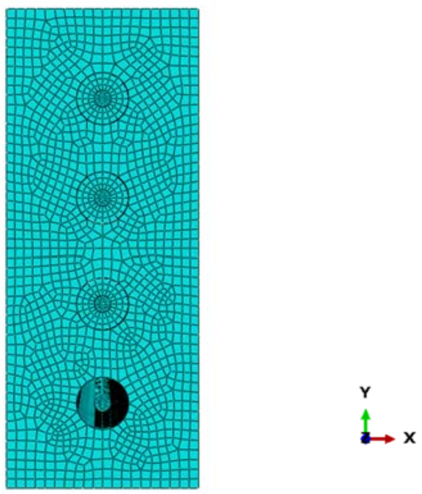

Figure 6. Side view of beam.

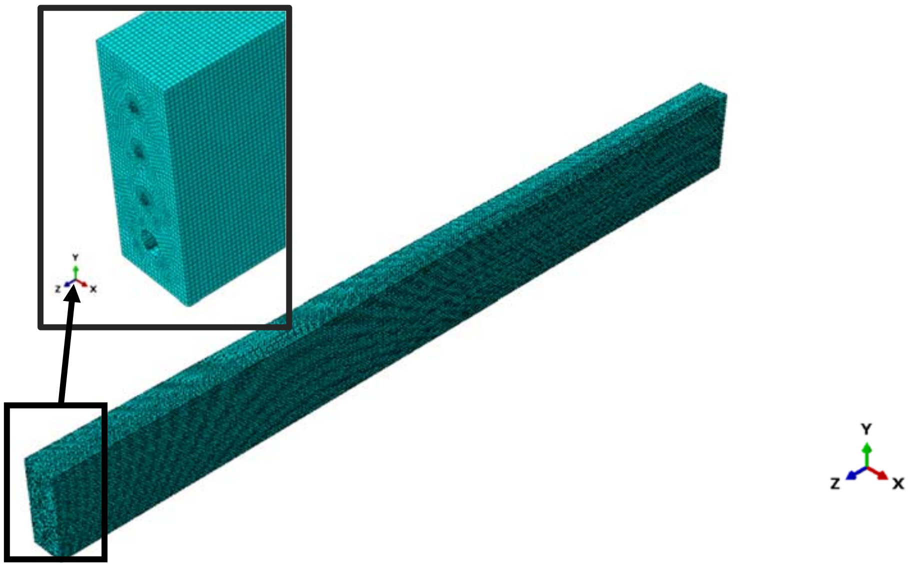

Figure 7. Overall diagram of beam.

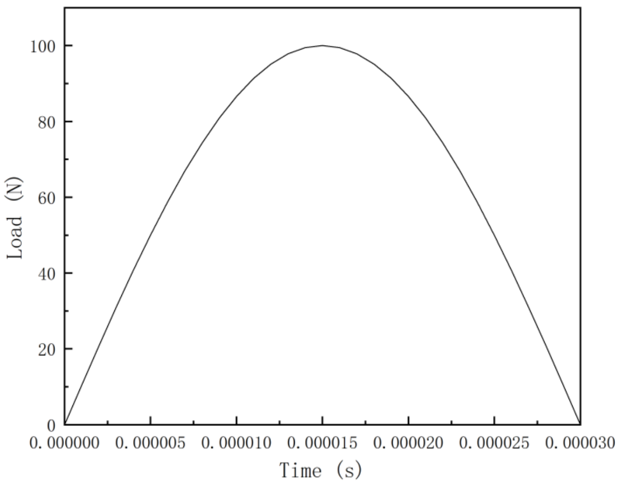

Figure 8. Half-sine periodic load.

3.2. Numerical Simulation Results

Simulations of hammering signals were conducted in the four pre-stressed pipes in the above model, and the received signals and their spectra in the different pipes were obtained. The results are as follows.

① Pipeline 1

The simulated signal of pipeline 1 is shown in Figure 9. The result of the spectral analysis is shown in Figure 10.

From Figures 9 and 10, the following can be concluded.

The simulated signal wave velocity of pipeline 1 is 4315.25 m/s, the peak frequency is 3680 Hz, and the maximum amplitude is 0.0171 m/s^2.

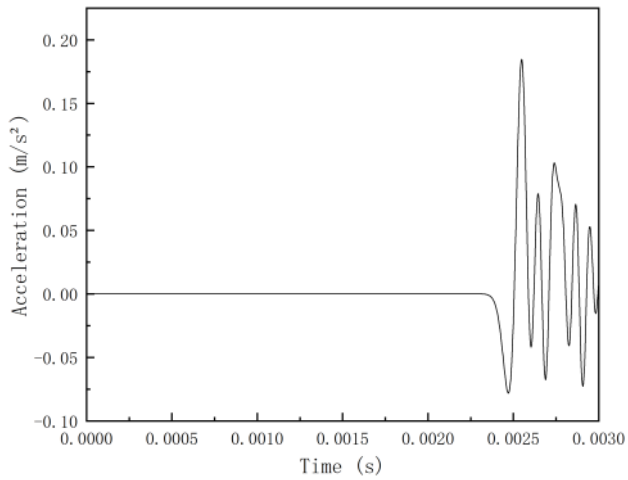

Figure 9. Simulated time history diagram of pipeline 1 signal.

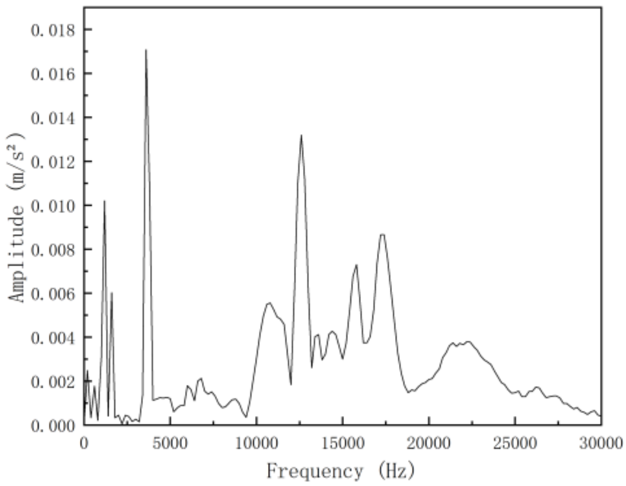

Figure 10. Simulated spectrum diagram of pipeline 1 signal.

② Pipeline 2

The simulated signal of pipeline 2 is shown in Figure 11. The result of the spectral analysis is shown in Figure 12.

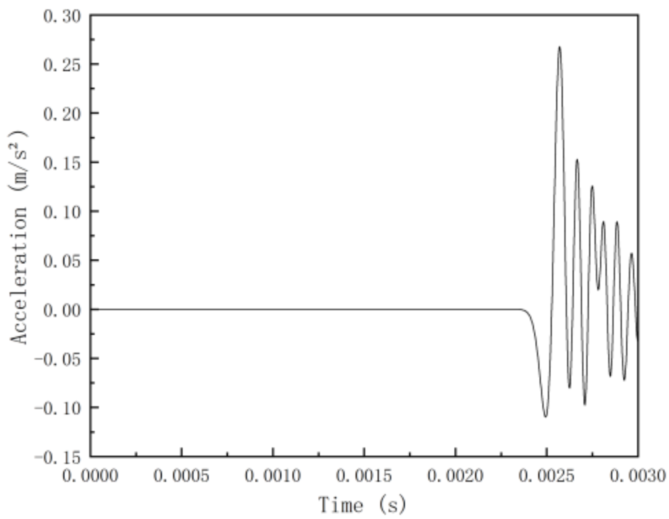

Figure 11. Simulated time history diagram of pipeline 2 signal.

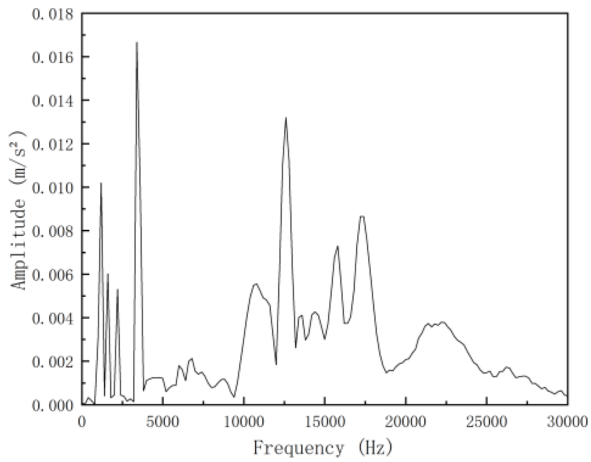

Figure 12. Simulated spectrum diagram of pipeline 2 signal.

From Figures 11 and 12, the following can be concluded.

The simulated signal wave velocity of pipeline 2 is 4276.57 m/s, the peak frequency is 3390 Hz, and the maximum amplitude is 0.0167 m/s^2.

③ Pipeline 3

The simulated signal of pipeline 3 is shown in Figure 13. The result of the spectral analysis is shown in Figure 14.

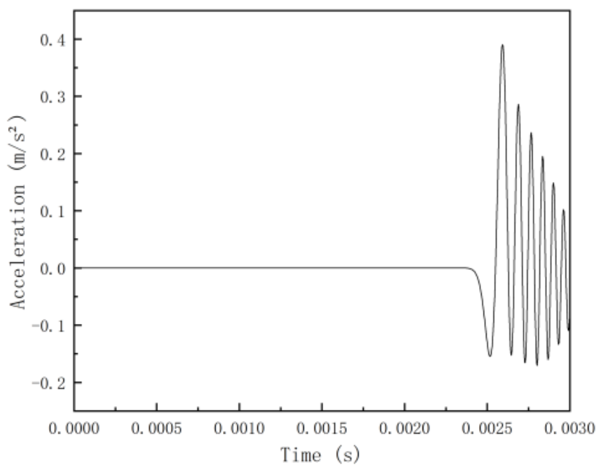

Figure 13. Simulated time history diagram of pipeline 3 signal.

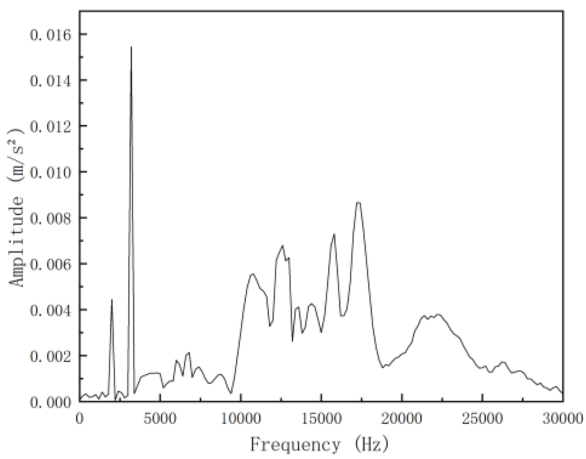

Figure 14. Simulated spectrum diagram of pipeline 3 signal.

From Figures 13 and 14, the following can be concluded.

The simulated signal wave velocity of pipeline 3 is 4243.96 m/s, the peak frequency is 3200 Hz, and the maximum amplitude is 0.0154 m/s^2.

④ Pipeline 4

The simulated signal of pipeline 4 is shown in Figure 15. The result of the spectral analysis is shown in Figure 16.

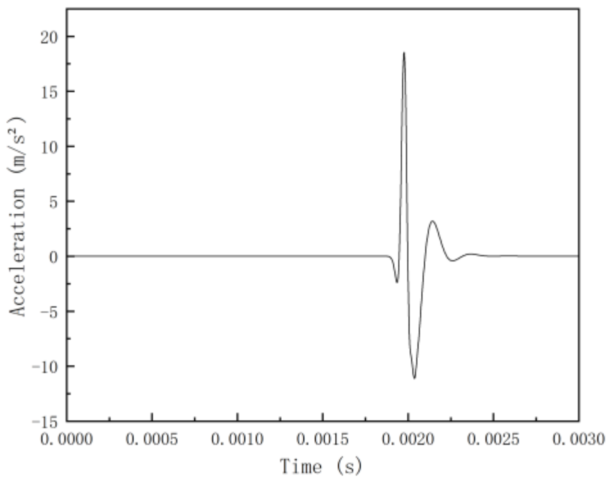

Figure 15. Simulated time history diagram of pipeline 4 signal.

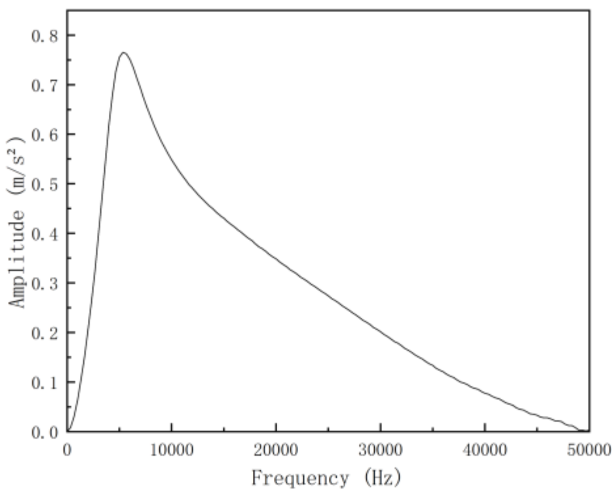

Figure 16. Simulated spectrum diagram of pipeline 4 signal.

From Figures 15 and 16, the following can be concluded.

The simulated signal wave velocity of pipeline 4 is v_4 = 5395.80 m/s, the peak frequency is f_4 = 6333 Hz, and the maximum amplitude is 0.793 m/s^2.

A summary of the data in Figures 9–16 is shown in Table 2.

Table 2. Numerical analysis of simulated signals.

Pipeline #	Wave Velocity (m/s)	Peak Frequency (Hz)	Maximum Amplitude (m/s^2)
1	4315.25	3680	0.0171
2	4276.57	3390	0.0167
3	4243.96	3200	0.0154
4	5395.80	6333	0.7930

In Table 2, it can be seen that in the analysis and comparison of the total void signals, the wave velocity attenuation amplitude of the N3 pipeline grouting compaction is 18.57%, and the peak frequency attenuation amplitude is 49.47% compared to that of the N4 pipeline without grouting, which is 18.57%. Additionally, the wave velocity attenuation amplitude of the N3 pipeline grouting compaction is 1.85% and 5.60% compared to the N2 pipeline, with a void of 0.5 m. In the comparison of multiple void signals, the wave velocity attenuation amplitude of 0.5 m of the N2 pipeline is 0.86%, and the peak frequency attenuation amplitude is 7.89% compared to the N1 pipeline with 1 m emptying.

It can be preliminarily concluded that the propagation speed of transmitted waves increases as the degree of slurry detachment increases, the attenuation of signal energy slows down, and the frequency shifts towards high frequencies. The quality of pre-stressed pipeline grouting can be preliminarily qualitatively analyzed from the perspectives of wave velocity, frequency transfer, and energy attenuation.

4. Analysis of Test Results

4.1. Result of Transmission Wave Test Method

The AGI-BWG instrument was used to test the hammering signals of the four pre-stressed pipes in the test beam. The test data and analysis results are as follows. The singular line is the excitation signal. The even-numbered line is the signal at the receiving end.

① Pipeline 1

The tested signal of pipeline 1 is shown in Figure 17. The result of the spectral analysis is shown in Figure 18.

The tested signal wave velocity of pipeline 1 is 4340 m/s, and the peak frequency is 3662 Hz.

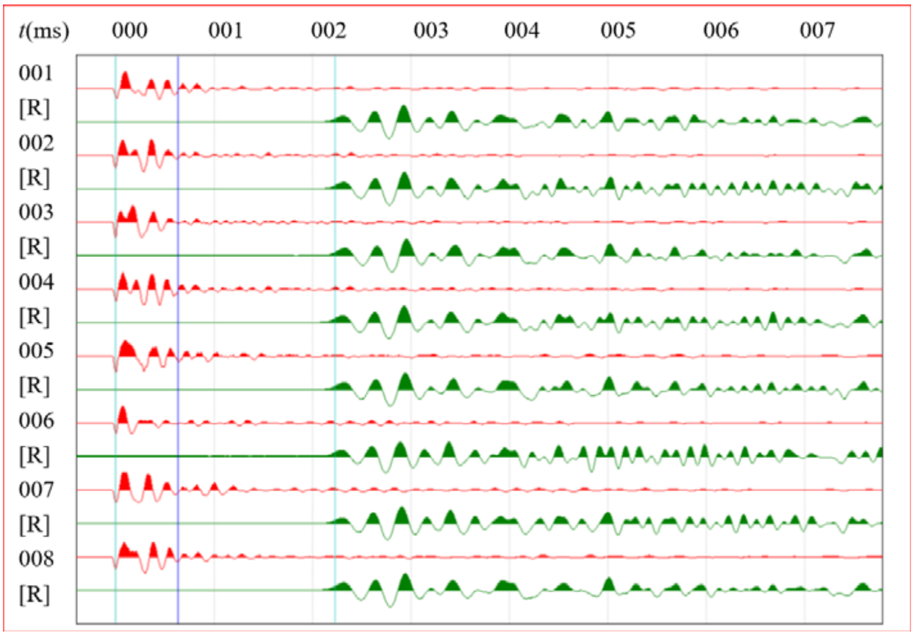

Figure 17. Tested time history diagram of pipeline 1 signal.

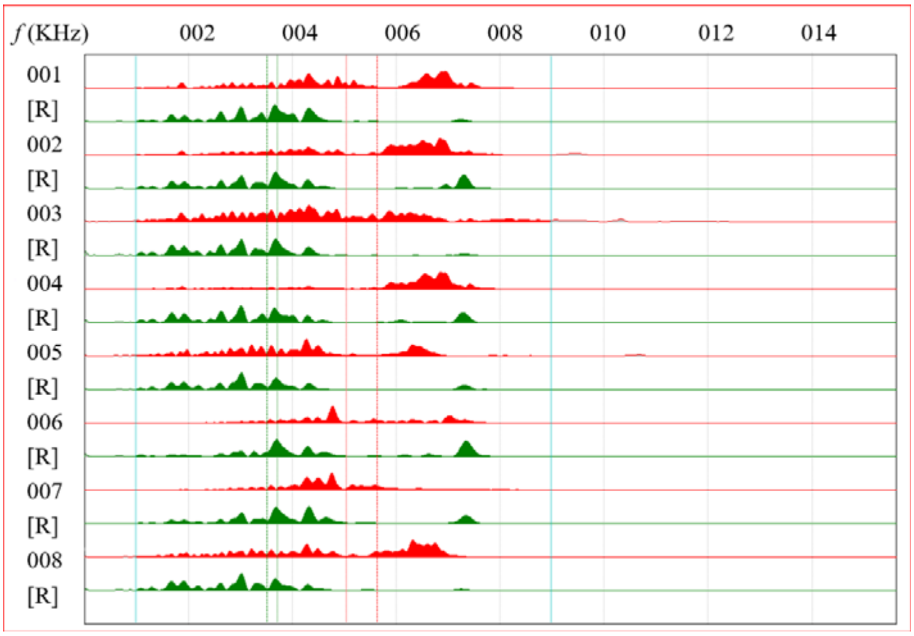

Figure 18. Tested spectrum diagram of pipeline 1 signal.

② Pipeline 2

The tested signal of pipeline 2 is shown in Figure 19. The result of the spectral analysis is shown in Figure 20.

The tested signal wave velocity of pipeline 2 is 4325 m/s, and the peak frequency is 3448 Hz.

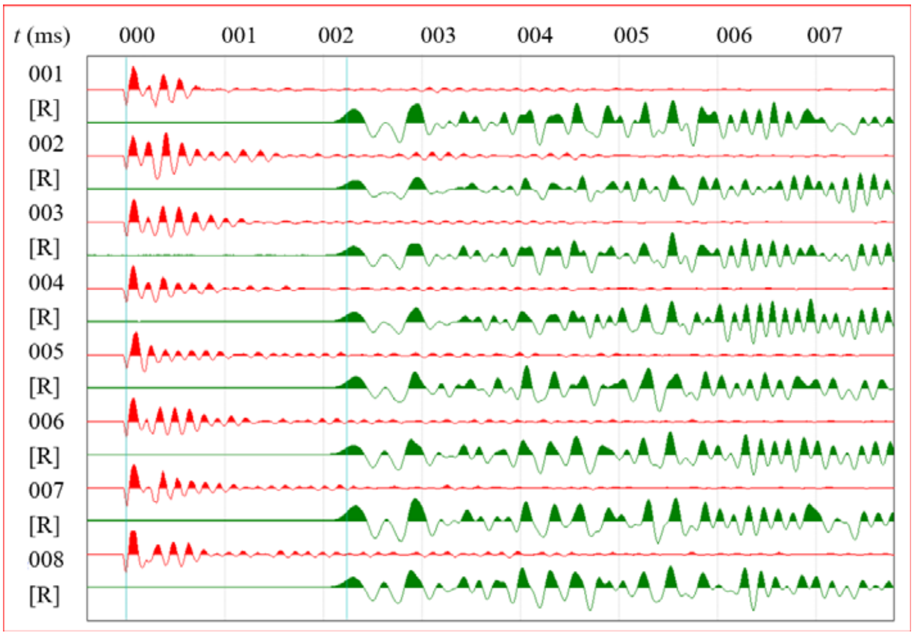

Figure 19. Tested time history diagram of pipeline 2 signal.

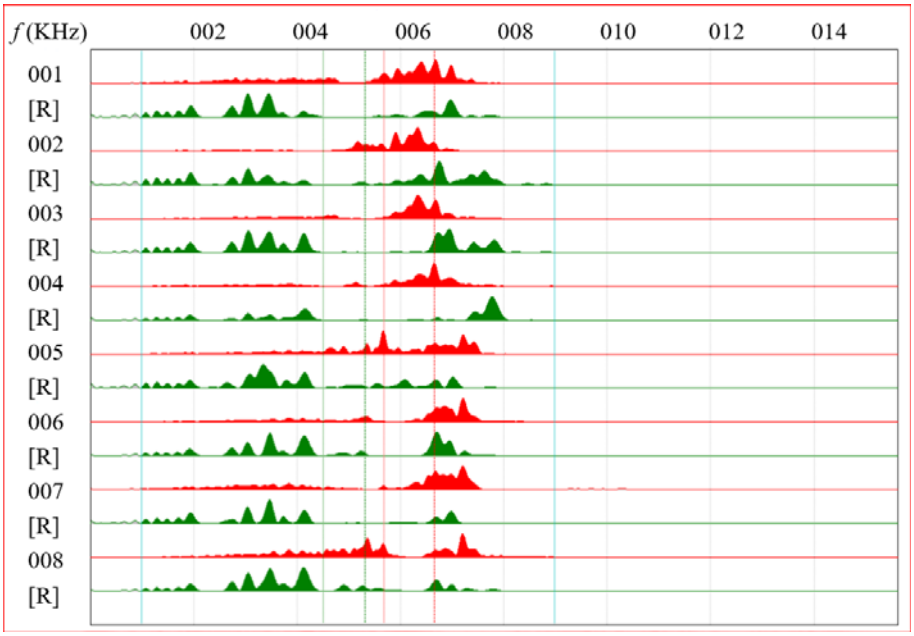

Figure 20. Tested spectrum diagram of pipeline 2 signal.

③ Pipeline 3

The tested signal of pipeline 3 is shown in Figure 21. The result of the spectral analysis is shown in Figure 22.

The tested signal wave velocity of pipeline 3 is 4310 m/s, and the peak frequency is 3143 Hz.

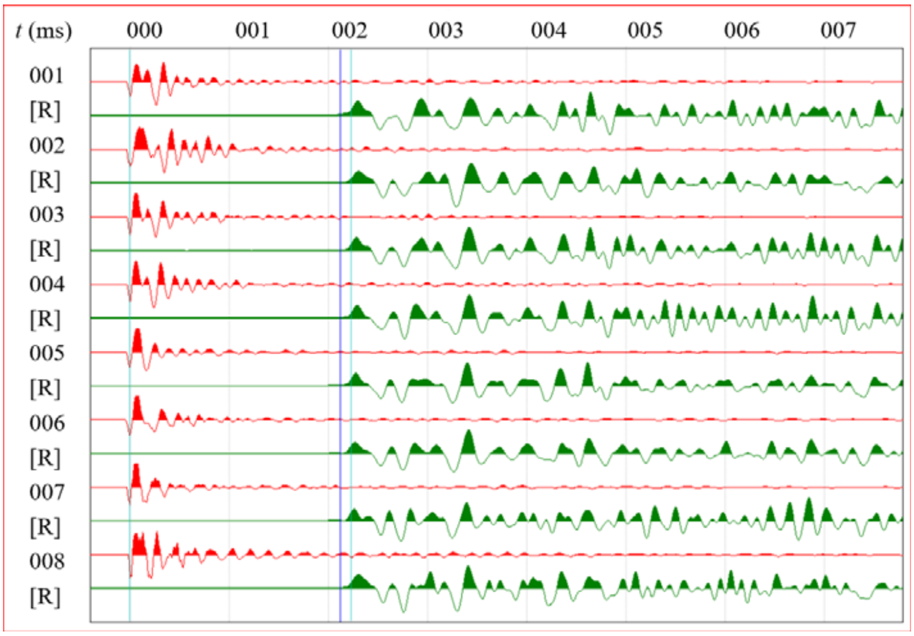

Figure 21. Tested time history diagram of pipeline 3 signal.

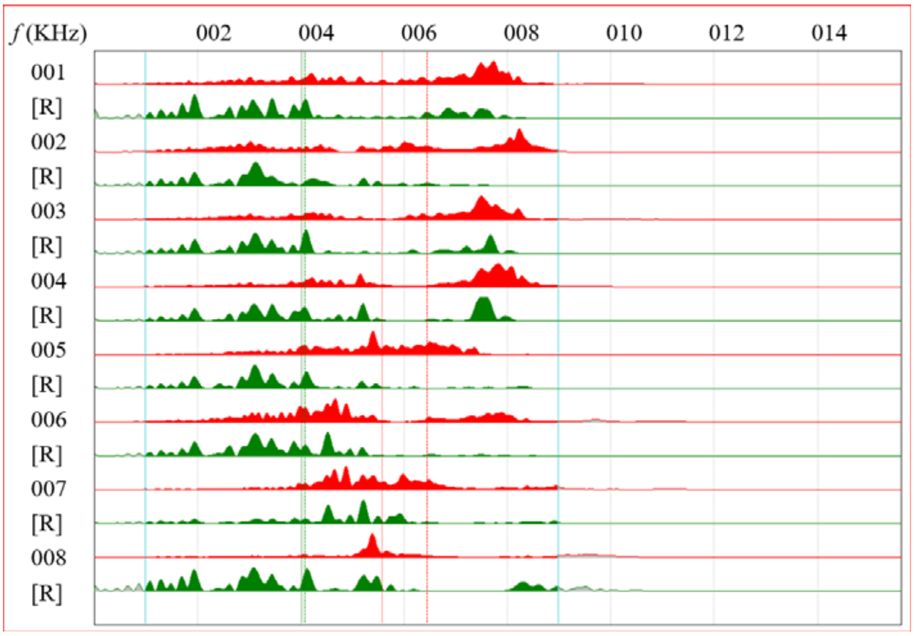

Figure 22. Tested spectrum diagram of pipeline 3 signal.

④ Pipeline 4

The tested signal of pipeline 4 is shown in Figure 23. The result of the spectral analysis is shown in Figure 24.

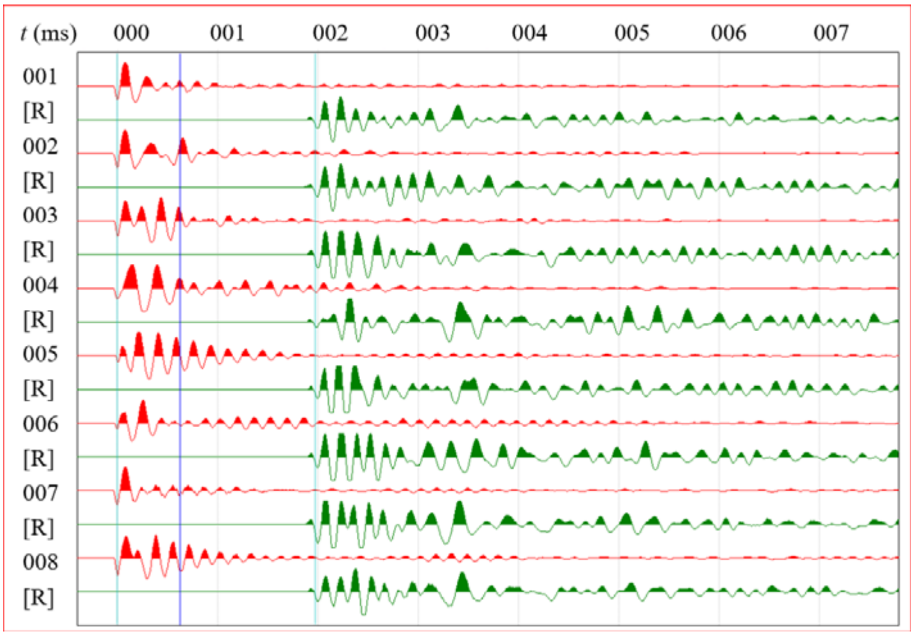

Figure 23. Tested time history diagram of pipeline 4 signal.

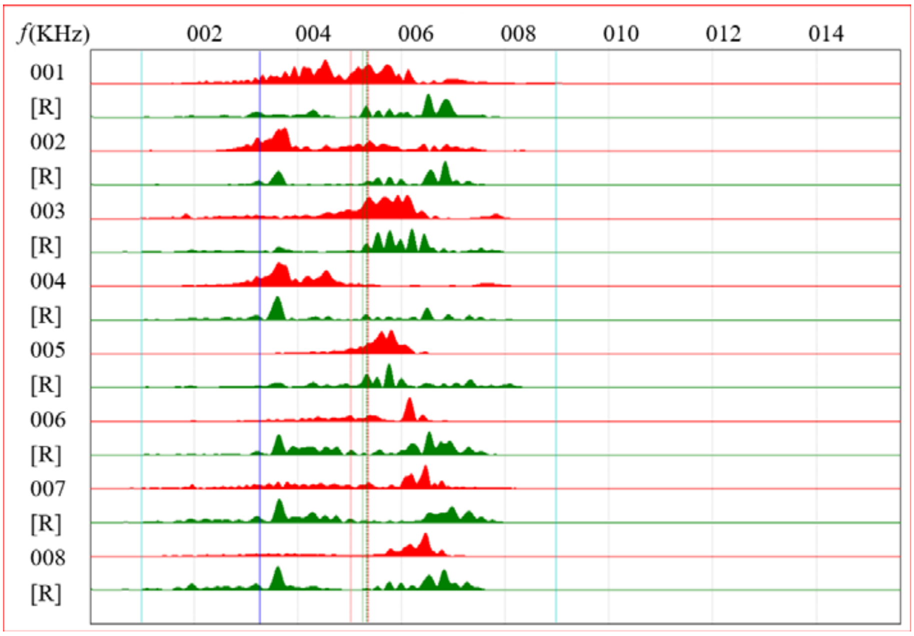

Figure 24. Tested spectrum diagram of pipeline 4 signal.

The tested signal wave velocity of pipeline 4 is 5274 m/s, and the peak frequency is 6516 Hz.

The test results in Figures 17–24 are summarized in Table 3. It can be seen that in the transmission wave test method, with the increase in the degree of slurry emptying, the propagation speed of the transmitted wave increases. The degree of signal energy attenuation slows down, and the frequency shifts towards high frequencies.

Table 3. The results of the tested signal.

Pipeline #	Wave Velocity (m/s)	Peak Frequency (Hz)
1	4340.00	3662
2	4325.00	3448
3	4310.00	3143
4	5274.00	6516

4.2. Comparison between Simulated Data and Experimental Data

Based on the above finite element analysis and actual test data, a summary is shown in Table 4.

Table 4. Signal comparison analysis.

Pipeline #	Wave Velocity (m/s)		Frequency (Hz)		Error %	
	Simulated	Tested	Simulated	Tested	Wave Velocity	Frequency
1	4315.25	4340.00	3680	3662	0.57	0.4
2	4276.57	4325.00	3390	3448	1.11	1.68
3	4243.96	4310.00	3200	3143	1.53	1.78
4	5395.80	5274.00	6333	6516	2.26	2.81

In Table 4, it can be seen that the simulation results of ABAQUS are consistent with the test data, and the errors vary between 0.4 and 2.81. Therefore, the simulation method of ABAQUS is reasonable and applicable. It was also found that the propagation speed of the transmitted wave increases as the degree of defects increases, and the frequency shifts towards high frequencies. It is known that the propagation velocity of elastic waves in pre-stressed steel is higher than that in concrete. Normally, the propagation velocity of elastic waves in pre-stressed steel is more than about 5000 m/s, and it is more than about 4000 m/s in concrete. The propagation velocity of elastic waves will be higher in pre-stressed pipelines, as there are more defects (slurry detachment). This is because elastic waves propagate in pre-stressed steel to a greater degree. The higher the propagation velocity of elastic waves, the lower the quality of the grouting in the pre-stressed pipeline (the more defects). The lower the propagation velocity of elastic waves, the higher the quality of the grouting in the pre-stressed pipeline. The propagation velocity of elastic waves in pre-stressed pipelines is an indicator of the quality of the grouting.

5. Conclusions

In this study, a full-scale model of a pre-stressed beam was constructed, and a pre-stressed pipe grouting quality detection system was used in conjunction with the simulation results of ABAQUS finite element software to conduct on-site validation tests. This approach provides a reliable means for detecting the quality of pre-stressed pipe grouting, and it can be widely applied in engineering practice. The main conclusions are as follows:

(1) This study aimed to investigate the feasibility of using the ultrasonic wave method to detect the grouting quality of pre-stressed pipelines. Through a combined approach of experiments and numerical simulations, we conducted in-depth research on the rapid qualitative assessment of defects using the ultrasonic wave method.
(2) The experimental results indicate that as the defect severity of pre-stressed pipelines increases, the propagation velocity of the elastic waves within the pipelines also increases, with a frequency shift towards higher frequencies. The propagation velocity of elastic waves within pre-stressed pipelines serves as an indicator of grouting quality.
(3) The consistency between the experimental and simulation results demonstrates that the ultrasonic wave method can, to some extent, evaluate the grouting quality of pre-stressed pipelines. This non-destructive and rapid detection method provided by the ultrasonic wave method offers a reliable means for assessing the grouting quality of pre-stressed pipelines.

Author Contributions: Conceptualization: Q.W. proposed the concept of quality inspection of pre-stressed pipeline grouting based on the transmission method, suggesting the use of numerical simulation and experimental verification; Methodology: Y.L. (Yun Luo) presented detailed methods and experimental procedures using numerical simulation; Software: Y.L. (Yang Liu) contributed to the article by conducting numerical simulations of the experiments using relevant software; Validation: M.S. conducted experimental verification of the method according to the design steps; Formal analysis ang writing-original draft: H.L. analyzed and evaluated the entire experimental method, and completed the initial draft of the write-up; Writing-review& editing: X.L. organized and edited the initial draft of the article. All authors have read and agreed to the published version of the manuscript.

Funding: This research received no external funding.

Institutional Review Board Statement: Not applicable.

Informed Consent Statement: Not applicable.

Data Availability Statement: The raw data supporting the conclusions of this article will be made available by the authors on request.

Conflicts of Interest: Authors Qingshan Wang and Yang Liu are employed by the China Construction Seventh Engineering Division Co., Ltd. Authors Yun Luo is employed by the Yunnan Jiaohang Engineering Technology Co., Ltd. Author Yang Liu is employed by the China Construction Seventh Engineering Division (Shanghai) Co., Ltd. The remaining authors declare that the research was conducted in the absence of any commercial or financial relationships that could be construed as a potential conflict of interest.

References

1. Rehman, S.K.U.; Ibrahim, Z.; Memon, S.A.; Jameel, M. Nondestructive test methods for concrete bridges: A review. *Constr. Build. Mater.* **2016**, *107*, 58–86. [CrossRef]
2. Martin, J.; Broughton, K.J.; Giannopolous, A.; Hardy, M.S.A.; Forde, M.C. Ultrasonic tomography of grouted duct post-tensioned reinforced concrete bridge beams. *NDT E Int.* **2001**, *34*, 107–113. [CrossRef]
3. Conner, J.M.; Pollock, D.G.; Khaleghi, B. Detection of Simulated Voids in Grouted Ducts using Groundpenetrating Radar//HPC: Build Fast, Build to Last. In Proceedings of the 2006 Concrete Bridge Conference, Reno, NV, USA, 7–10 May 2006.
4. Olson, L.D.; Tinkey, Y. Impact echo scanning for imaging of grout defects to mitigate corrosion in post-tensioned bridge ducts. *Struct. Health Monit. Intell. Infrastruct.* **2006**, *1–2*, 539–544.
5. Brachelet, F.; Du, T.; Defer, D.; Antczak, E. Detection of Poor Filling in Pre-Stressed Beams Specimen by Inductive Thermography and Transfer Function Analysis. In Proceedings of the 7th International Symposium on Non-destructive Testing in Civil Engineering, Nantes, France, 30 June–3 July 2009.
6. Chai, H.K.; Aggelis, D.G.; Momoki, S.; Kobayashi, Y.; Shiotani, T. Single-side access tomography for evaluating interior defect of concrete. *Constr. Build. Mater.* **2010**, *24*, 2411–2418. [CrossRef]
7. Ohtsu, M.; Alver, N. Development of non-contact SIBIE procedure for identifying ungrouted tendon duct. *NDT E Int.* **2009**, *42*, 120–127. [CrossRef]
8. Osawa, S.; Shiotani, T.; Kitora, H.; Momiyama, Y. Damage Visualization of Imperfectly-Grouted Sheath in PC Structures. In Proceedings of the 31st Conference of the European Working Group on Acoustic Emission (EWGAE), Dresden, Germany, 3–5 September 2014; pp. 1–8.
9. Lu, J. Quality Analysis of Grout in Post-Tensioned Bridge Ducts and Study on Nondestructive Testing Methods. Master's Thesis, Hunan University, Beijing, China, 2017.
10. Guo, Z. Research on Grout Transmission Method Detection of Pre-stressed Holes Based on BP Neural Network. Ph.D. Thesis, Zhengzhou University, Henan, China, 2022.
11. Freij, H.; Dukeman, D.; Alexander, C.L.; Ruffolo, M.D.; Frigerio, T.; Boselli, J.; Mariscotti, M.A.; Sagüés, A.A. Comparison of novel imaging sensor and gamma ray tomography imaging of grout deficiencies in external post-tensioned structural tendons. *NDT E Int.* **2021**, *117*, 102368. [CrossRef]
12. Wang, S. Research on the Grouting Quality Detection Technology of Tendon Ducts Based on Impact-Echo Method. Ph.D. Thesis, Zhengzhou University, Henan, China, 2023.
13. Li, W.J.; Ho, S.C.M.; Patil, D.; Song, G.B. Acoustic emission monitoring and finite element analysis of debonding in fiber-reinforced polymer rebar reinforced concrete. *Struct. Health Monit.* **2017**, *11*, 674–681. [CrossRef]
14. Zhu, Z.; Mi, S.; Lu, G.; Wang, F.; Zhou, Y. Numerical simulation of ultrasonic detection for grouting quality of metal prestressed ducts. *J. Cent. South Univ. (Nat. Sci. Ed.)* **2012**, *43*, 4888–4894.
15. Shakor, P.; Gowripalan, N.; Rasouli, H. Experimental and numerical analysis of 3D printed cement mortar specimens using inkjet 3DP. *Arch. Civ. Mech. Eng.* **2021**, *3*, 58. [CrossRef]
16. Zeng, H.; Xiao, B.; Xu, Z.; Wang, Y.; Su, J. Research on Frequency Shift Method for Locating Grouting Defects in Bridge Pre-stressed Pipeline. *J. Eng. Geophys.* **2014**, *11*, 254–259.
17. Zeng, H. Development and Application of a Quality Testing Instrument for Grouting of Bridge Pre-stressed Pipeline. Master's Thesis, Yangtze University, Hubei, China, 2015.